2009 American Control Conference
Hyatt Regency Riverfront, St. Louis, MO, USA
June 10-12, 2009

Control-Oriented Aerothermoelastic Modeling Approaches for Hypersonic Vehicles

Adam J. Culler, Jack J. McNamara, and Andrew R. Crowell

Abstract— **The field of aerothermoelasticity is essential for control-oriented modeling of hypersonic vehicles due to a high degree of coupling between vehicle systems, as well as the presence of aerodynamic heating. In the present study, an efficient aerothermoelastic model is investigated in two ways. First, an approximate aerodynamic heating model is verified using Computational Fluid Dynamic flow analysis. Next, the model is used to gain insight into the degree of coupling between the aerothermal and aeroelastic systems. Results demonstrate that both material property degradation and two-way coupling are important for control-oriented aerothermoelastic modeling. Furthermore, quasi-static and dynamic average approaches for fluid-thermal-structural coupling offer an accurate and efficient approximation for implementing two-way coupling.**

NOMENCLATURE

c	plate specific heat
c_f	local skin friction coefficient
D	$= Eh^3/12(1-\nu^2)$, bending stiffness
E	modulus of elasticity
H	enthalpy
h	plate thickness
k	plate thermal conductivity
L	plate length, streamwise
M	Mach number
M_T	thermal moment
N_x	in-plane load, total
Pr	Prandtl number
p	pressure
Q_{aero}	aerodynamic heat flux
Q_{rad}	radiation heat flux
q_a	$= p - p_\infty$, aerodynamic pressure
q_∞	$= \rho_\infty U_\infty^2/2$, dynamic pressure
Re	Reynolds number
St	Stanton number
T	temperature
T_{env}	environment temperature
t	time
U	air velocity
w	normal plate displacement
x	streamwise coordinate
z	normal coordinate
α	thermal expansion coefficient
γ	ratio of specific heats, air
ϵ	emissivity
ν	Poisson's ratio
ρ	air density
ρ_m	plate density
σ	Stefan-Boltzmann constant

Subscripts

∞	freestream
aw	adiabatic wall
e	edge of the boundary layer
w	wall

Superscripts

$*$	reference enthalpy condition

A.J. Culler is a Ph.D. candidate in the Department of Aerospace Engineering, The Ohio State University, Columbus, OH 43210, USA culler.40@osu.edu

J.J. McNamara is an Assistant Professor in the Department of Aerospace Engineering, The Ohio State University, Columbus, OH 43210, USA mcnamara.190@osu.edu

A.R. Crowell is a Graduate Research Assistant in the Department of Aerospace Engineering, The Ohio State University, Columbus, OH 43210, USA crowell.25@osu.edu

I. INTRODUCTION

Currently, there is a focus by NASA, the United States Department of Defense, and the United States Air Force on the development of hypersonic technologies for next generation reusable launch vehicles and unmanned hypersonic cruise vehicles [1]-[5]. As shown in Fig. 1, modern hypersonic vehicle configurations are typically based on a lifting body, integrated airframe-propulsion concept, where the entire lower vehicle surface is part of a scramjet engine. A challenge with this class of vehicle is a tight-coupling between the aerodynamic, control, structural, and propulsion systems that cannot be neglected during analysis and design [5]-[10]. Furthermore, air-breathing hypersonic vehicles must fly within the atmosphere for sustained periods of time to meet the needs of the propulsion system [7], [11]; resulting in severe aerodynamic heating.

These issues imply that the field of aerothermoelasticity, which involves mutual fluid-thermal-structural interactions in a system, has an important role in *control-oriented* modeling of hypersonic vehicles[5]. Specifically, structural deflections alter the inflow to the engine, as well as the flow over the outer body; while the stiffness and aeroelastic behavior of the vehicle and control effectors are time and mission dependent. Thus, the incorporation of aerothermoelastic effects is essential to successful guidance, navigation, and control of hypersonic vehicles systems [12]. During the last 15 years, a number of researchers have performed investigations into these effects using multi-disciplinary models of hypersonic vehicles [5], [13]-[28]. This study aims to expand upon this work by improving *control-oriented* aerothermoelastic

978-1-4244-4524-0/09/$25.00 ©2009 AACC

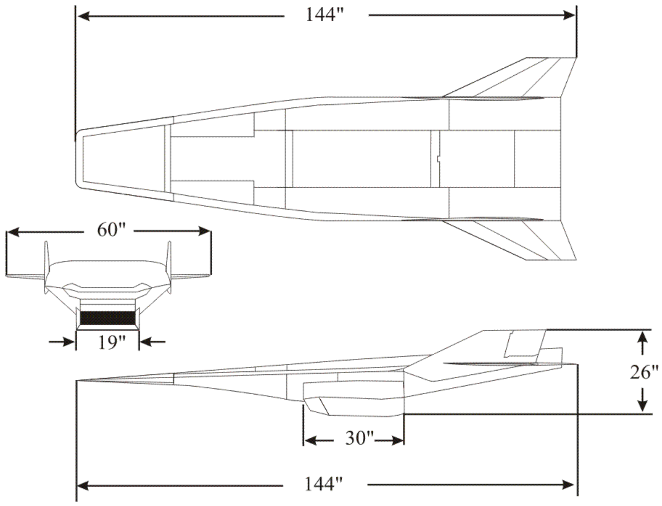

Fig. 1. Schematic of the NASA X-43 Experimental Aircraft.

modeling approaches. The objective of this study is to investigate an efficient procedure for computing the aerodynamic heating on hypersonic vehicles appropriate for control design and evaluation, and characterize the degree of coupling between the fluid-thermal-structural interactions. Since this is a preliminary investigation, a relatively simple configuration is chosen; namely a flexible panel on the surface of a hypersonic vehicle.

II. Method of Solution

The aerothermoelastic modeling approach used in this study is illustrated in Fig. 2. The aerothermal problem consists of interaction between the aerodynamic heating and structural heat transfer, while the aeroelastic problem consists of fully-coupled inertial-elastic-aerodynamic interactions. The coupled aerothermoelastic model includes the influence of aerodynamic heating on structural deformation (Mechanism 1) and feedback from the aeroelastic solution to the aerothermal problem (Mechanism 2).

A. Fluid Model

The panel considered in this study is located on an inclined surface of a wedge-shaped body, as shown in Fig. 3. The

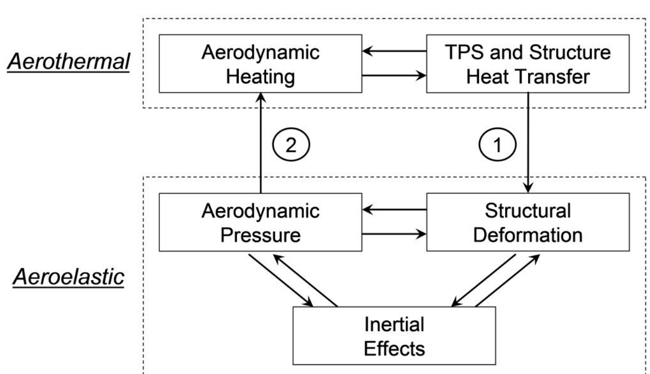

Fig. 2. Fully-coupled modeling approach for aerothermoelastic systems.

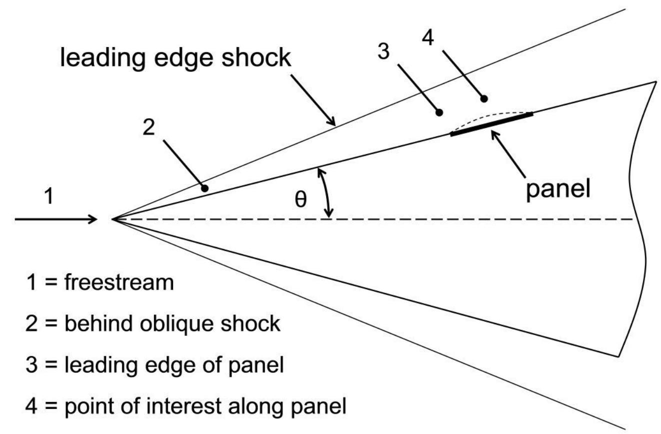

Fig. 3. Panel located on an inclined surface of a wedge-shaped body.

inclined surface before and after the panel is assumed to be flat and rigid, thus the inviscid flow properties at the leading edge of the panel (Location 3) are the same as those behind the leading edge shock [29].

The unsteady inviscid pressure over the panel is computed using third order piston theory [30], which has been used extensively in hypersonic aeroelastic research [12]. Since the panel is located on an inclined surface, the "freestream" flow conditions used in (1) to compute the pressure distribution over the panel are those at the leading edge of the panel. The inviscid flow temperature and Mach number distributions near the panel are computed using isentropic flow relations [29] based on the total condition at the leading edge of the panel and the pressure distribution from (1).

$$
\begin{aligned}
q_a = 2\frac{q_\infty}{M_\infty}\Bigg[\left(\frac{1}{U_\infty}\frac{\partial w}{\partial t} + \frac{\partial w}{\partial x}\right) + \frac{\gamma+1}{4}M_\infty\left(\frac{1}{U_\infty}\frac{\partial w}{\partial t}\right. \\
\left. + \frac{\partial w}{\partial x}\right)^2 + \frac{\gamma+1}{12}M_\infty^2\left(\frac{1}{U_\infty}\frac{\partial w}{\partial t} + \frac{\partial w}{\partial x}\right)^3\Bigg]
\end{aligned}
\tag{1}
$$

Aerodynamic heating is modeled using Eckert's reference enthalpy method [31]. The reference enthalpy method uses boundary layer equations from incompressible flow theory, but with flow properties evaluated at a reference enthalpy to account for the effects of compressibility. Using reference parameters, heat flux at the wall, Q_{aero}, is given by (2). For turbulent flow the Stanton number, St^*, is determined using the Colburn-Reynolds analogy shown in (3), and the local skin frictin coefficient, c_f^*, is calculated using the Schultz-Grunow formula given in (4) [31]. Coupling from the structure to the aerodynamic heating model is achieved by updating the edge flow properties as the structure deforms, and also by updating the surface temperature of the panel as it is heated.

$$Q_{aero} = St^* \rho^* U_e (H_{aw} - H_w) \tag{2}$$

$$St^* = \frac{c_f^*}{2}\frac{1}{(Pr^*)^{2/3}} \tag{3}$$

$$c_f^* = \frac{0.370}{(\log_{10} Re_x^*)^{2.584}} \quad (4)$$

B. Thermal Model

Transient temperature distributions in the panel, $T(x, z, t)$, are computed using the two-dimensional heat equation (5) to include both chordwise and through-thickness conduction paths. The thermal model includes both a thermal protection system (TPS) and the plate structure. The TPS is modeled as thermal insulation with a high-emissivity upper surface. The boundary condition along the upper surface includes aerodynamic heating, $Q_{aero}(x, t)$, from (2), and thermal radiation, $Q_{rad}(x, t)$, given by (6). Thermal radiation is modeled by considering the upper surface to be non-black, diffuse, and enclosed by the environment [32]. An adiabatic boundary condition is applied to the lower surface and edges of the panel.

$$\rho_m c \frac{\partial T}{\partial t} = k_x \frac{\partial^2 T}{\partial x^2} + k_z \frac{\partial^2 T}{\partial z^2} \quad (5)$$

$$Q_{rad} = \sigma\epsilon(T^4 - T_{env}^4) \quad (6)$$

C. Structural Model

The panel structure is shown graphically in Fig. 4 and is modeled using *von Kármán* plate theory [33], [34] with (7), which includes in-plane thermal force, thermal moment, and unsteady aerodynamic pressure. Chordwise variation of the elastic modulus, $E(x)$, and the thermal expansion coefficient, $\alpha(x)$, are included. The panel is supported by immovable, simple supports and only transverse vibrations are considered.

$$D\frac{\partial^4 w}{\partial x^4} - N_x\frac{\partial^2 w}{\partial x^2} + h\rho_m\frac{\partial^2 w}{\partial t^2} + q_a + \frac{\partial^2 M_T}{\partial x^2} = 0 \quad (7)$$

D. Coupled Aerothermoelastic Panel Solution

The panel deformation is computed using Galerkin's method [34], [35] in conjunction with a fourth order Runge-Kutta time-integration procedure [36]. An explicit finite difference approach [32], [37] is used to solve the heat equation; transient temperatures in the panel are computed at discrete points through the thickness and along the length.

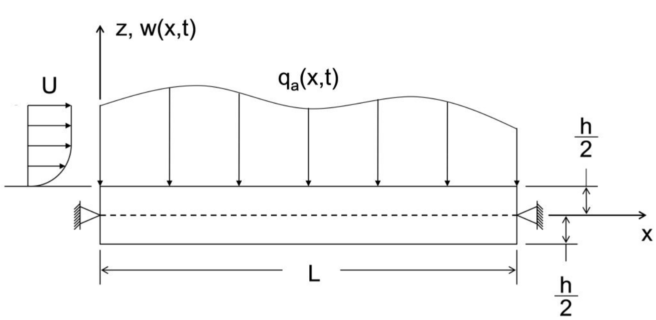

Fig. 4. Simply supported plate structure.

III. Results

A. Verification of the Reference Enthalpy Model

In order to characterize the accuracy of the reference enthalpy model (REM), a computational fluid dynamic (CFD) flow analysis is used to compute the heating over a representative vehicle surface at a representative operating condition. The CFD code chosen for this analysis is the NASA Langley CFL3D code [38]. This code solves the Reynolds-averaged Navier-Stokes (RANS) equations. Four different turbulence models were used in the present study, namely: 1) Baldwin-Lomax [39] (BL), 2) Spalart-Allmaras [40] (SA), 3) Wilcox $k-\omega$ [41] (WX), and 4) Menter's $k-\omega$ SST [42] (MT). Note that the accuracy of these turbulence models in the hypersonic regime was evaluated in [43], [44].

The geometry chosen for this verification study is based on a 2-D vehicle configuration used at the Air Force Research Laboratory (AFRL) to develop a comprehensive hypersonic vehicle model [5]. Only the forebody of the vehicle is considered here. The computational grid is shown in Fig. 5. The computational domain is a 2 x 585 x 157 H-H grid with 273 points on the upper surface and 257 points on the lower surface. The operating condition and flow properties used for this verification study are listed in Table I.

A comparison of the aerodynamic heat flux computed using the REM and a CFD flow analysis is illustrated in Fig. 6. The different models yield qualitatively similar results where the aerodynamic heat flux peaks at the leading edge and decreases along the surface. The REM yields the lowest aerodynamic heat flux, and most closely agrees with the Baldwin-Lomax prediction. In general, the Baldwin-Lomax and Wilcox $k-\omega$ models yield the lower and upper bounds, respectively, of the CFD computations. The notable exception is the Spalart-Allmaras result, which predicts an extended laminar region relative to the other models. Over the upper surface of the vehicle, the REM is within 15% of the Baldwin-Lomax prediction, and 30% of the Wilcox $k-\omega$

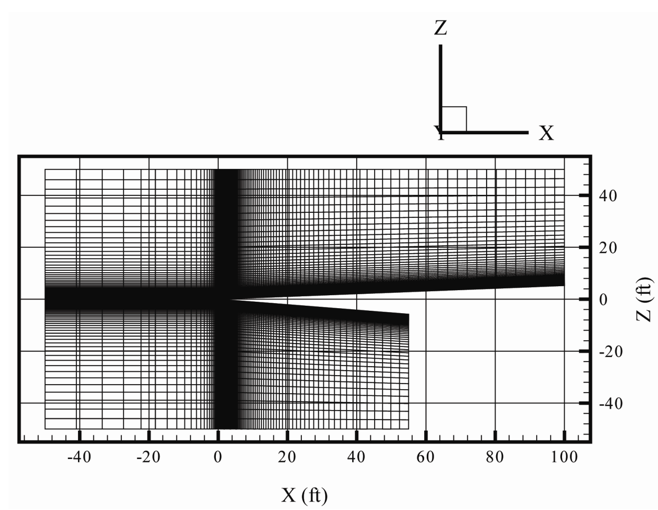

Fig. 5. Computational grid for the forebody of an air-breathing hypersonic vehicle geometry.

prediction. Over the lower surface, the agreement is slightly better. Specifically, the REM is within 10% of the Baldwin-Lomax prediction, and 25% of the Wilcox $k-\omega$ prediction. Note that the average percent variation between the Baldwin-Lomax and Wilcox $k-\omega$ predictions is 21% over the upper surface, and 19% over the lower surface. Therefore, the percent difference between the REM relative to the CFD models is on the same order as the percent variation between the different CFD models. Based on these results, the REM is considered appropriate for the current application. Control design using this model, however, must account for at least 30% uncertainty in the predicted aerodynamic heat flux.

B. Fluid-Thermal-Structural Coupling

In order to assess the degree of fluid-thermal-structural coupling in hypersonic flow, the dynamic stability boundary (aka flutter boundary) of the panel was computed using several different cases listed in Table II. Cases 'B' correspond to the neglect of material property degradation in the analysis. Cases 'B' and 'C' utilize quasi-static fluid-thermal-structural coupling, i.e. the panel deformation is computed without inertial terms in the equation of motion. The temperature distribution is then frozen, and panel stability is determined from a response test of the system using the fully dynamic equations of motion. Cases 'D' solve the dynamic equations of motion, therefore panel stability is inherently included in the solution. A '1' corresponds to one-way aerothermal-aeroelastic coupling, while '2' corresponds to two-way coupling. Case 'D-2' represents a tightly coupled solution to the complete dynamic equations, thus this case is considered the "truth model." The 'D-3' case represents a solution procedure where the aeroelastic and aerothermal solutions are marched forward in time on separate time scales (several time steps of aeroelastic simulation per one time step of aerothermal simulation). The dynamic response of the panel deformation is averaged and passed to the aerothermal solution to update the aerodynamic heating.

While normal operation of hypersonic vehicles avoid operation near or beyond the onset of flutter, computation of the boundary provides a convenient single metric for assessing the importance of fluid-thermal-structural coupling. The parameters used in the panel analysis is listed in Table III. Temperature dependent material properties of the thermal insulation [45] and the titanium plate [46], [47] are included.

Several important observations related to control-oriented aerothermoelastic modeling can be made from Fig. 7. It is evident by comparing the 'B' cases to the 'C' and 'D' cases that inclusion of material property degradation (e.g. softening

TABLE I
HYPERSONIC VEHICLE ANALYSIS PARAMETERS.

Altitude	25.9 km
Mach Number	8.0
Angle of Attack	2.0^o
Wall Temperature	1389 K
Reynold's Number	1.714e6

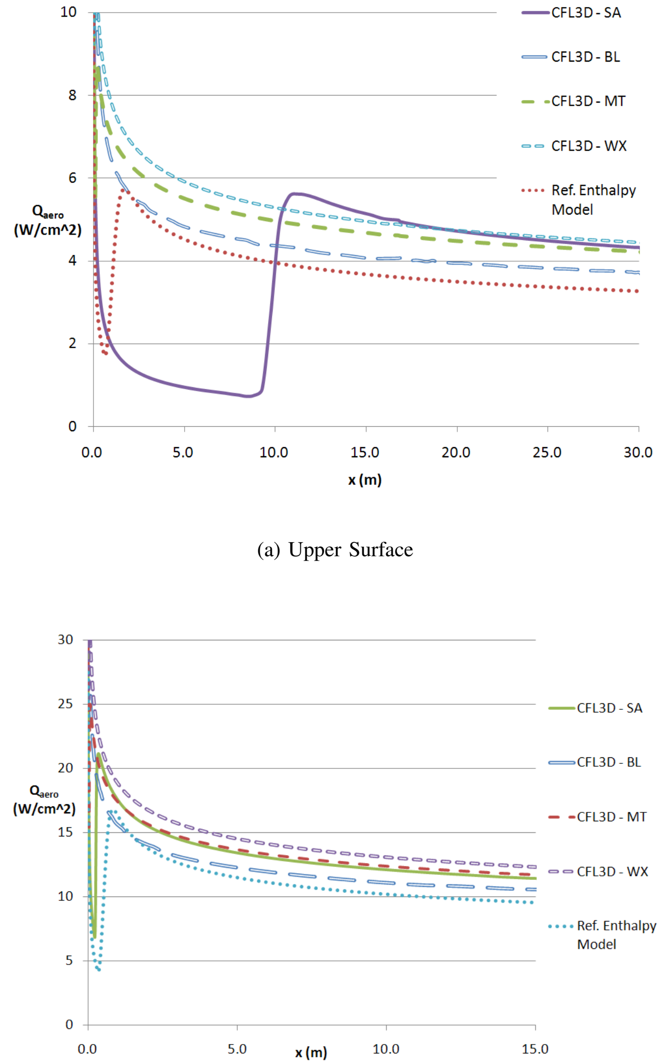

(a) Upper Surface

(b) Lower Forebody Surface

Fig. 6. Comparison of the aerodynamic heat flux over the hypersonic vehicle geometry, computed using CFD and the reference enthalpy model.

of the structure due to heating) is important for aerothermoelastic modeling over extended trajectories. Furthermore, note that there is little difference between the time to onset of panel flutter for the one-way versus two-way coupling solutions for the high Mach number cases. However there are significant differences in time to onset of flutter for the lower Mach numbers considered. This can be attributed with the fact that for lower Mach numbers the panel is farther from dynamic instability. It takes longer operation in hypersonic flow for aerodynamic heating to degrade the panel to the onset of flutter. Thus two-way coupling is an important effect for extended exposure of structures to hypersonic flows, where errors introduced through one-way thermal coupling increase with time. These lower Mach number results are most applicable for control-oriented aerothermoelastic modeling since air-breathing hypersonic vehicles will operate for extended periods of time under exposure to aerodynamic heating. Finally, note that both the quasi-static and dynamic averaged cases produce excellent agreement with the 'D-2' case. These approaches to fluid-thermal-structural coupling are 170 and 26 times faster, respectively, than a one-to-one time stepped, dynamic solution for the aerothermoelastic problem. An issue with the quasi-static case, however, is evident for the Mach 8.0 operating condition, where the nonlinear equation solver failed to converge to a solution. Therefore, for cases with linear or moderately nonlinear deformations, the quasi-static fluid-thermal-coupling strategy may be satisfactory. For moderate to high nonlinear deformations, the dynamic averaged approach may be required.

TABLE II
AEROTHERMOELASTIC MODELING CASES.

Case	Coupling Type	Aeroheating Panel Shape	Material Degradation	Aerothermoelastic Simulation
B-1	1-way	Flat	None	Quasi-Static
B-2	2-way	Inst. Def.	None	Quasi-Static
C-1	1-way	Flat	$E(T)$, $\alpha(T)$	Quasi-Static
C-2	2-way	Inst. Def.	$E(T)$, $\alpha(T)$	Quasi-Static
D-1	1-way	Flat	$E(T)$, $\alpha(T)$	Dynamic
D-2	2-way	Inst. Def.	$E(T)$, $\alpha(T)$	Dynamic
D-3	2-way	Avg. Def.	$E(T)$, $\alpha(T)$	Dynamic

TABLE III
AEROTHERMOELASTIC PANEL FLUTTER STUDY PARAMETERS.

Altitude	30 km
Freestream Mach Number	8 – 14
Nondimensional Dynamic Pressure	73 – 203
Forebody Surface Inclination	5.0°
Transition to Turbulence Upstream of Panel	1.0 m
Panel Length	1.5 m
Plate Thickness	5.0 mm
Initial Panel Temperature	300 K

IV. Conclusions and Future Work

Control-oriented modeling in the hypersonic regime requires coupling aerothermal and aeroelastic systems. The fully-coupled aerothermoelastic model used in this study incorporates the reference enthalpy method for aerodynamic heating. The reference enthalpy method is shown to be in good agreement with 2-D CFD flow analysis at the representative operating condition, and is computationally efficient. Aerothermoelastic simulation illustrate that the effects of material property degradation and two-way thermal coupling is important for control-oriented modeling of hypersonic vehicles. The latter requirement implies significant penalties in computational expense of aerothermoelastic modeling. However two approaches are introduced that significantly reduce this expense, namely quasi-static or dynamic averaged fluid-thermal-structural coupling. Future work will extend the aerothermoelastic modeling approach used here to a three-dimensional vehicle to further explore these effects on a more representative configuration.

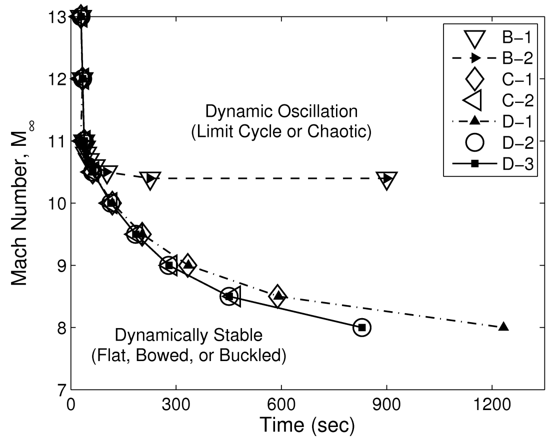

(a) Comparison of flutter boundaries for the aerothermoelastic modeling cases.

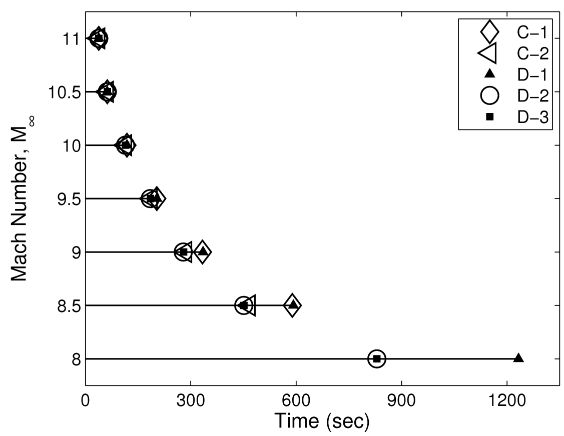

(b) Comparison of flight time to the onset of flutter

Fig. 7. Aerothermoelastic flutter boundary predictions.

V. Acknowledgments

This research is funded in part by NASA award NNX08AB32A with Mr. Peter Ouzts as technical monitor, an AFRL summer research fellowship with Dr. David Doman as technical monitor, and by a National Defense Science and Engineering Graduate Fellowship to Adam Culler.

References

[1] Mansour, N., Pittman, J., and Olson, L., "Fundamental Aeronautics Hypersonics Project: Overview," *39th AIAA Thermophyscis Conference*, 2007, AIAA Paper 2007-4263.

[2] Walker, W. and Rodgers, F., "Falcon Hypersonic Technology Overview," *13th International Space Planes and Hypersonic Systems and Technologies Conference*, Capua Italy, 2005, AIAA 2005-3253.

[3] Kazmar, R., "Airbreathing Hypersonic Propulsion at Pratt & Whitney - Overview," *13th AIAA/CIRA International Space Planes and Hypesonics Systems and Technologies Conference*, Capua, Italy, May 16-20 2005, AIAA Paper 2005-3256.

[4] Dolvin, D.J., "Hypersonic International Flight Research and Experimentation (HIFiRE) Fundamental Sciences and Technology Development Strategy," *Proceedings of the 15th AIAA International Space Planes and Hypersonic Systems and Technologies Conference*, Dayton, OH, April 2008, AIAA Paper No. 2008-2581.
[5] Bolender, M. and Doman, D., "Nonlinear Longitudinal Dynamical Model of an Air-Breathing Hypersonic Vehicle," *Journal of Spacecraft and Rockets*, Vol. 44, No. 2, March - April 2007.
[6] Cazier, F.W., Doggett, R.V., and Ricketts, R.H., "Structural Dynamic and Aeroelastic Considerations for Hypersonic Vehicles," *Proc. 32th AIAA/ASME/ASCE/AHS/ASC Structures, Structural Dynamics and Materials Conference*, Baltimore, MD, April 8-10 1991.
[7] Anderson, J.D., *Hypersonic and High Temperature Gas Dynamics*, McGraw-Hill, New York, 1989.
[8] Blankson, IM., "Air-Breathing Hypersonic Waveriders: A Survey of Research Needs," *Proceedings of the First International Waverider Symposium*, University of Maryland, College Park, MD, October 1990.
[9] Bertin, J.J. and Cummings, R.M., "Fifty Years of Hypersonics: Where We've Been and Where We're Going," *Progress in Aerospace Sciences*, Vol. 39, April 2003, pp. 511–536.
[10] Fidan, B., Mirmirani, M., and Ioannou, P., "Flight Dynamics and Control of Air-Breathing Hypersonic Vehicles: Review and New Directions," *12th AIAA International Space Planes and Hypersonic Systems and Technologies*, Norfolk, VA, 2003, AIAA Paper No. 2003-7081.
[11] Bertin, J.J., *Hypersonic Aerothermodynamics*, AIAA, 1994.
[12] McNamara, J.J., Friedmann, P.P., Powell, K.G., Thuruthimattam, B.J., and Bartels, R.E., "Aeroelastic and Aerothermoelastic Behavior in Hypersonic Flow," *AIAA Journal*, Vol. In Press, 2008.
[13] Schmidt, D., "Dynamics and Control of Hypersonic Aeropropulsive/Aeroelastic Vehicles," AIAA Paper No. 92-5326-CP.
[14] Heeg, J. and Gilbert, M.G., "Active Control of Aerothermoelastic Effects for a Conceptual Hypersonic Aircraft," *Journal of Aircraft*, Vol. 30, 1993, pp. 453–458.
[15] Chavez, F. and Schmidt, D., "Uncertainty Modeling For Multivariable-Control Robustness Analysis of Elastic High-Speed Vehicles," *Journal of Guidance, Control, and Dynamics*, Vol. 22, No. 1, 1999.
[16] Lind, R., "Linear Parameter-varying Modeling and Control of Structural Dynamics with Aerothermoelastic Effects," *Proc. 40th AIAA/ASME/ASCE/AHS/ASC Structures, Structural Dynamics, and Materials Conference and Exhibit*, St. Louis, MO, 1999, AIAA Paper 99-1393.
[17] Lind, R., Buffington, J., and Sparks, A., "Multi-loop Aeroservoelastic Control of a Hypersonic Vehicle," *AIAA Guidance, Navigation, and Control Conference and Exhibit*, Portland, OR, 1999, AIAA Paper 99-4123.
[18] Rudd, L. and Pines, D., "Integrated Propulsion Effects on Dynamic Stability and Control of Hypersonic Waveriders," *Proc. 36th AIAA/ASME/SAE/ASEE Joint Propulsion Conference and Exhibit*, Huntsville, AL, July 1990, AIAA Paper 2000-3826.
[19] Mirmirani, M., Wu, C., Clark, A., Choi, S., and Colgren, R., "Modeling for Control of a Generic Air-Breathing Hypersonic Vehicle," *AIAA Guidance, Navigation, and Control Conference and Exhibit*, San Fransisco, CA, August 2005, AIAA Paper 2005-6256.
[20] Fidan, B., Kuipers, M., Ioannou, P., and Mirmirani, M., "Longitudinal Motion Control of Air-Breathing Hypersonic Vehicles Based on Time-Varying Models," *14th AIAA International Space Planes and Hypersonic Systems and Technologies Conference*, Canberra, AUS, 2006, AIAA Paper No. 2006-8074.
[21] Raney, D., McMinn, J., Pototzky, A., and Wooley, C., "Impact of Aeroelasticity on Propulsion and Longitudinal Flight Dynamics of an Air-Breathing Hypersonic Vehicle," *Proceedings of the 34th AIAA/ASME/ASCE/AHS/ASC Structures, Structural Dynamics and Materials Conference*, La Jolla, CA, April 19-22 1993, pp. 628 – 637, AIAA Paper 93-1367.
[22] Bolender, M. and Doman, D., "Modeling Unsteady Heating Effects on the Structural Dynamics of a Hypersonic Vehicle," *AIAA Atmospheric Flight Mechanics Conference and Exhibit*, Keystone, CO, August 2006, AIAA Paper 2006-6646.
[23] Oppenheimer, M. and Doman, D., "A Hypersonic Vehicle Model Developed With Piston Theory," *AIAA Atmospheric Flight Mechanics Conference and Exhibit*, Keystone, CO, August 2006, AIAA Paper 2006-6637.
[24] Williams, T., Bolender, M., Doman, D., and Morataya, O., "An Aerothermal Flexible Mode Analysis of a Hypersonic Vehicle," *AIAA Atmospheric Flight Mechanics Conference and Exhibit*, Keystone, CO, August 2006, AIAA Paper 2006-6647.
[25] Groves, K.P., Sigthorsson, D.O., Serrani, A., Yurkovich, S., Bolender, M., and Doman, D., "Reference Command Tracking for a Linearized Model of an Air-Breathing Hypersonic Vehicle," *AIAA Guidance, Navigation, and Control Conference and Exhibit*, San Fransisco, CA, August 2005, AIAA Paper 2005-6144.
[26] Groves, K.P., Serrani, A., Yurkovich, S., Bolender, M., and Doman, D., "Anti-Windup Control for an Air-Breathing Hypersonic Vehicle Model," *AIAA Guidance, Navigation, and Control Conference and Exhibit*, Keystone, CO, 2006, AIAA Paper 2006-6557.
[27] Sigthorsson, D.O., Serrani, A., Yurkovich, S., Bolender, M., and Doman, D., "Tracking and Control for an Overactuated Hypersonic Air-Breathing Vehicle with Steady-State Constraints," *AIAA Guidance, Navigation, and Control Conference and Exhibit*, Keystone, CO, 2006, AIAA Paper 2006-6558.
[28] Parker, J.T., Serrani, A., Yurkovich, S., Bolender, M., and Doman, D., "Control-Oriented Modeling of an Air-Breathing Hypersonic Vehicle," *Journal of Journal of Guidance, Control, and Dynamics*, Vol. In Press, 2007.
[29] Anderson, Jr, J. D., *Modern Compressible Flow with Historical Perspective*, McGraw-Hill, New York, 3rd ed., 2003.
[30] Ashley, H. and Zartarian, G., "Piston Theory - A New Aerodynamic Tool for the Aeroelastician," *Journal of the Aeronautical Sciences*, Vol. 23, No. 12, December 1956, pp. 1109–1118.
[31] Eckert, E. R. G., "Engineering Relations for Heat Transfer and Friction in High-Velocity Laminar and Turbulent Boundary-Layer Flow Over Surfaces With Constant Pressure and Temperature," *Transactions of the ASME*, Vol. 78, No. 6, August 1956, pp. 1273–1283.
[32] Holman, J. P., *Heat Transfer*, McGraw-Hill, New York, 8th ed., 1997.
[33] Thornton, E. A., *Thermal Structures for Aerospace Applications*, American Institute of Aeronautics and Astronautics, Reston, Virginia, 1996.
[34] Dowell, E. H., "Nonlinear Oscillations of a Fluttering Plate," *AIAA Journal*, Vol. 4, No. 7, July 1966, pp. 1267–1275.
[35] Hodges, D. H. and Pierce, G. A., *Introduction to Structural Dynamics and Aeroelasticity*, Cambridge University Press, Cambridge, New York, 2002.
[36] Chapra, S. C. and Canale, R. P., *Numerical Methods for Engineers: With Programming and Software Applications*, McGraw-Hill, New York, 3rd ed., 1998.
[37] Tannehill, J. C., Anderson, D. A., and Pletcher, R. H., *Computational Fluid Mechanics and Heat Transfer*, Taylor and Francis, Philadelphia, 2nd ed., 1997.
[38] Krist, S.L., Biedron, R.T., and Rumsey, C.L., "CFL3D User's Manual (Version 5.0)," NASA TM 1998-208444, 1997.
[39] Baldwin, B.S. and Lomax, H., "Thin Layer Approximation and Algebraic Model for Separated Turbulent Flows," Huntsville, AL, AIAA Paper 78-257, 1978.
[40] Spalart, P.R. and Allmaras, S.R., "A One-Equation Turbulence Model for Aerodynamic Flows," Reno, NV, AIAA Paper 92-0439, 1992.
[41] Wilcox, D., *Turbulence Modeling for CFD*, DCW Industries, Inc., La Canada, CA, 1993.
[42] Menter, F. and Rumsey, C., "Assessment of Two-Equation Turbulence Models for Transonic Flows," AIAA 94-2343, 1994.
[43] Sinha, K., Mahesh, K., and Candler, G., "Modeling the Effect of Shock Unsteadiness in Shock/Turbulent Boundary-Layer Interactions," *AIAA Journal*, Vol. 43, No. 3, March, 2005, pp. 586–594.
[44] MacLean, M., Wadhams, T., Holden, M., and Johnson, H., "A Computational Analysis of Ground Test Studies of the HIFiRE-1 Transition Experiment," *46th AIAA Aerospace Sciences Meeting and Exhibit*, AIAA 2008-641, 2008.
[45] Myers, D. E., Martin, C. J., and Blosser, M. L., "Parametric Weight Comparison of Advanced Metallic, Ceramic Tile, and Ceramic Blanket Thermal Protection Systems," NASA TM-2000-210289, June 2000.
[46] Williams, S. D. and Curry, D. M., "Thermal Protection Materials: Thermophysical Property Data," NASA RP-1289, December 1992.
[47] MIL-HDBK-5J, "Metallic Materials and Elements for Aerospace Vehicle Structures," Department of Defense, January 2003.